

A Search for Nitrogen Enriched Quasars in the Sloan Digital Sky Survey Early Data Release

Misty C. Bentz and Patrick S. Osmer

Department of Astronomy, The Ohio State University

140 W. 18th Ave, Columbus, OH 43210-1173

`bentz,posmer@astronomy.ohio-state.edu`

ABSTRACT

A search for nitrogen-rich quasars in the Sloan Digital Sky Survey Early Data Release (SDSS EDR) catalog has yielded 16 candidates, including five with very prominent emission, but no cases with nitrogen emission as strong as in Q0353-383. The quasar Q0353-383 has long been known to have extremely strong nitrogen intercombination lines at $\lambda 1486$ and $\lambda 1750$ Å, implying an anomalously high nitrogen abundance of ~ 15 times solar. It is still the only one of its kind known. A preliminary search through the EDR using the observed property of the weak C IV emission seen in Q0353-383 resulted in a sample of 23 objects with unusual emission or absorption-line properties, including one very luminous $z \approx 2.5$ star-forming galaxy. We present descriptions, preliminary emission-line measurements, and spectra for all the objects discussed here.

Subject headings: galaxies: active — galaxies: starburst — quasars: emission lines — surveys

1. Introduction

Q0353-383 was first observed in 1976 as part of the Curtis Schmidt survey (Osmer & Smith 1980). Subsequent observations of this $z = 1.96$ quasar revealed that Q0353-383 was an unusual object, in that its spectrum revealed prominent N III], N IV] and N V emission lines and abnormally weak C III] and C IV lines compared to other quasars. Figure 1a shows the spectrum of Q0353-383 (Baldwin, private communication) compared to the SDSS composite spectrum in Figure 1b (Vanden Berk et al. 2001). Osmer (1980) concluded that Q0353-383 has an anomalously high N abundance due to recent CNO processing in stars. Building on Osmer's original work with Q0353-383, Baldwin et al. (2003) obtained higher quality spectra and added HST observations in the ultraviolet. Using the latest models of the broad line region, Baldwin et al. were able to both confirm and refine the original conclusions made by Osmer. Additionally, Baldwin et al. conclude that Q0353-383 has a metallicity of at least 5-10 times solar. As shown by simulations (Hamann & Ferland 1999), this level of over abundance is expected to occur near the end of an era of rapid

metal enrichment which can result in metallicities of as much as 10-20 times solar. The scarcity of objects like Q0353-383 may be an indication of the amount of time a quasar spends in this state of extreme metal enrichment before the gas supply is exhausted and the quasar becomes inactive.

To date, Q0353-383 is the only object of its kind known, which brings up two questions: (1) how many other such objects exist, and (2) what percentage of the QSO population is similar to Q0353-383? Until recently, answering these questions was difficult due to the relatively small number of known quasars and the lack of available spectra with good S/N. However, the Sloan Digital Sky Survey (SDSS) is providing new opportunities by working to compile, in one database, approximately 100,000 quality quasar spectra as it scans 10,000 deg² of the north Galactic cap (York et al. 2000). Even though the survey is not complete at this time, a search for similar nitrogen-rich QSOs can be undertaken.

2. Spectral Analysis

The SDSS EDR (Stoughton et al. 2002) Quasar Catalog (Schneider et al. 2002) is composed of 3814 objects that cover an area on the sky of 494 deg². Three thousand of these objects were discovered by the SDSS in the commissioning data using a multicolor selection technique similar to the one described by Richards et al. (2002). Each object has at least one emission line with a full width half-maximum of more than 1000 km s⁻¹, a luminosity brighter than $M_{i^*} = -23$ mag, and a reliable redshift (Schneider et al. 2002). The sample is not homogeneous, as there were several modifications to the quasar selection algorithm during the time the data was collected, and so the EDR quasar catalog is not intended for statistical purposes. However, there are still enough data contained in the catalog to make the information mined there important.

The SDSS EDR database was searched for all quasars that lay within the redshift range $1.8 < z < 4.1$. This range ensures that both N IV] $\lambda 1486$ and N III] $\lambda 1750$ will be in the 3800–9200 Å region observed by the SDSS spectrograph. A total of 1082 QSOs were found in this range, with the redshift distribution as shown in Figure 2. We used the redshift values as specified in the Quasar Catalog (Schneider et al. 2002) to correct for cosmological expansion and place the spectra in a common rest frame. Within each spectrum, two 30 Å sections, centered on N IV] $\lambda 1486$ and N III] $\lambda 1750$, were cross-correlated with the rest-frame spectrum of Q0353-383 using the IRAF¹ package *fxcor*. The cross-correlation routine was good at picking out objects with relatively strong nitrogen emission, but it was also adept at finding noise. Therefore, objects with high correlation coefficients (> 0.3) for either species of nitrogen were visually inspected in order to verify the presence or absence of nitrogen emission. All objects with typical broad absorption line profiles were immediately discounted.

¹IRAF is distributed by the National Optical Astronomy Observatories, which are operated by the Association of Universities for Research in Astronomy, Inc., under cooperative agreement with the NSF.

We detected sixteen candidate nitrogen-rich objects within our sample of 1082 quasars. While the sixteen objects selected had a correlation coefficient of at least 0.5 for either N III] or N IV] (see Table 2), five of the candidates have noticeably stronger nitrogen emission than the others (SDSS J1308–0050, SDSS J1327+0035, SDSS J1744+5351, SDSS J2326–0020, and SDSS J2336–0017; see Table 2), but none have nitrogen emission from both species as strong as that seen in Q0353-383. The SDSS spectrum of each object, smoothed over five pixels, is shown in Figure 3. Five of the sixteen candidate quasars were known previous to the SDSS; however, only one (SDSS J0034-0111, aka UM 259) was noted as possibly having strong nitrogen emission (MacAlpine et al. 1977).

2.1. Description of Candidates

Due to the faintness of the objects, the spectra are somewhat noisy, and so the equivalent widths of emission lines in this paper should be taken as guideline measurements, with a characteristic error of 0.5-1 Å. The measurements were made using a simple summing function and a two-point interpolation of the continuum within IRAF (see Table 2). None of the objects presented here have nitrogen lines as strong as in Q0353-383. Many of the candidates do not even have an obvious N IV] emission line, but this could, in part, be due to the noise at the blue edge of the spectra for the $z \approx 2$ quasars.

In the cases of the two quasars where Ly α emission is visible in the EDR spectra (SDSS J0953+0037 and SDSS J1707+6443, Figures 3g and 3m, respectively), the line profile is rather narrow with a well-separated N V emission line. This is also true of Q0353-383. A literature search on the previously known quasars revealed that SDSS J0259-0020 (Chaffee et al. 1991, Fig. 1; Osmer et al. 1994, Fig.1) and SDSS J1238-0059 (Hewett et al. 1991, Fig. 1) also follow this trend. However, SDSS J1442-0037 (Hewett et al. 1991, Fig. 2m) has a somewhat broader Ly α profile with nearly indistinguishable N V emission, and SDSS J0034-0111 (Osmer et al. 1994, Fig. 2k) has a very broad, blended Ly α and N V line profile.

There appear to be narrow components as well as broad components to the emission line profiles in several of the spectra. In fact, the FWHM of the C IV line ranges from $\sim 800 \text{ km s}^{-1}$ (SDSS J0953+0037, Fig. 3g) to $\sim 7000 \text{ km s}^{-1}$ (SDSS J0250-0047 and SDSS J2336-0017, Figs. 3d and 3q) within the sample of 16 quasars. SDSS J0953+0037 is extremely strange in that it appears to be a narrow-line QSO with many intrinsic Ly α and C IV absorbers. It also happens to be the one case where an [O I] night sky line fell exactly at $\lambda 1750$, and so it is impossible to determine if there is N III] emission using the SDSS spectrum.

Of additional interest, seven of the candidates have strong, well-separated He II $\lambda 1640$ and O III] $\lambda 1664$ emission lines (see Table 3), which is another of the odd characteristics of Q0353-383. There is evidence for He II and O III] emission in most of the other spectra, but the S/N are too low for even preliminary measurements of these weak lines.

The overall continuum shapes of the candidates are also rather varied. Three candidates have a

relatively flat continuum, six have a slight slope to the blue in the continuum that is shortward of the C III] emission line, and the remaining seven have a distinct slope to the blue throughout the visible portion of their spectra. About one-third of the candidate quasars also seem to have absorption signatures, although only one seems to have a broad absorption profile (SDSS J1327+0035).

While it appears that most of the candidates are clustered right around $z \approx 2$, this is to be expected as the distribution of quasar redshifts in the SDSS EDR peaks near this redshift.

3. Other Findings

As noted by Osmer & Smith (1980), the C IV/(Ly α + N V) ratio of Q0353-383 is extremely small, a value of 0.07, which is 4 to 5 times smaller than the average value of the other quasars in the Curtis Schmidt survey. Therefore, as a preliminary search, those quasars in the SDSS EDR database with a (non-negative) ratio of C IV/(Ly α + N V) < 0.1 were examined. The C IV/(Ly α + N V) ratios were calculated using the crude equivalent widths supplied by the EDR pipeline, which included the effects of absorption and/or emission. Table 4 lists the properties of the 23 QSOs matching these criteria, none of which were previously known. Interestingly, the two nitrogen-rich candidates SDSS J0953+0037 and SDSS J1707+6443 have redshifts greater than 2.3 (where Ly α shifts into the SDSS spectrograph window of 3800–9200 Å), and yet they were not among the 23 quasars that were selected (see Figure 4 for spectra). This particular search technique was not very useful for our purposes, but it did a nice job of collecting extremely peculiar objects, with broad absorption lines, intrinsic C IV and N V absorption, strong narrow Ly α emission with well-separated N V emission, and even one high-redshift star-forming galaxy. Two objects (SDSS J1303+0020 and SDSS J1426-0021, Figures 4k and 4p, respectively) show evidence for strong outflows with P-Cygni (narrower than normal BALs) line profiles of N V, C IV, and the Si blend at λ 1400.

3.1. A Star-Forming Galaxy Candidate at $z \approx 2.5$

One of the objects uncovered in our search, SDSS J1432-0001, was included in the EDR quasar catalog on account of its strong Ly α emission and UV brightness. This object, however, seems to be a starburst galaxy (see Figure 5 for comparison with the composite Lyman break galaxy (LBG) spectrum from Shapley et al. 2003). There is strong evidence for the following interstellar absorption features in the spectrum of SDSS J1432-0001: Si II λ 1260, O I λ 1302, Si II λ 1304, C II λ 1334, Si IV λ 1393, 1402, Si II λ 1526, C IV λ 1548, 1550, Fe II λ 1608, Al II λ 1670, and Al III λ 1854, 1862 (Shapley et al. 2003; Morton 1991). The continuum of SDSS J1432-0001 is redder than that of the LBG composite, and the lines are somewhat broader as well. Also, there seems to be very little intergalactic absorption immediately shortward of Ly α . However, while slightly different, SDSS J1432-0001 has many of the same emission- and absorption-line features of the LBG composite,

and it has similar colors to the LBGs of the Steidel et al. (2003) LBG survey, with $u^* - g^* = 2.03$ and $g^* - r^* = 0.6$.

SDSS J1432-0001 has an observed r^* magnitude of 20.52, which is two magnitudes brighter than the brightest LBG in the Steidel et al. (2003) survey (Q0201-oMD12 at $z = 2.567$ has an \mathcal{R}_{AB} magnitude of 22.67), and four magnitudes brighter than typical $z \approx 3$ LBGs, which have magnitudes of $\mathcal{R}_{AB} = 24 - 25.5$ mag (Shapley et al. 2003). SDSS imaging of SDSS J1432-0001 shows no evidence for a foreground lensing galaxy, although this cannot be ruled out as the SDSS data are insufficient to determine the presence of sub-arcsecond image splitting or the presence of a foreground lensing system at $z \approx 1$.

If we assume, however, that the continuum emission at $\lambda 1500 \text{ \AA}$ arises only from young O and B stars, we can estimate the star formation rate (SFR) of the galaxy from the flux at $\lambda 1500 \text{ \AA} \times (1 + z)$ ($F_\lambda(1500)$), which was measured directly from the calibrated spectrum and has a value of $F_\lambda(1500) \approx 2.2 \times 10^{-17} \text{ erg s}^{-1} \text{ cm}^{-2} \text{ \AA}^{-1}$. The flux was converted to luminosity assuming a cosmological model with $\Omega_M = 0.3$, $\Omega_\Lambda = 0.7$, and $h = 0.7$. Assuming a Salpeter IMF with mass limits of 0.1 to 100 M_\odot and a 10^8 year old continuous star formation model, Kennicutt (1998) derives the relation

$$\text{SFR } M_\odot \text{ yr}^{-1} = 1.4 \times 10^{-28} L_\nu(\lambda 1500) \quad (1)$$

between the star formation rate and the luminosity density L_ν (in $\text{ergs s}^{-1} \text{ Hz}^{-1}$) at $\lambda = 1500 \text{ \AA}$. The implied SFR is therefore $\sim 390 M_\odot \text{ yr}^{-1}$, without correction for attenuation by dust. “Normal” spiral galaxies have typical SFRs of $0 - 5 M_\odot \text{ yr}^{-1}$ (Barbaro & Poggianti 1997), and the LBGs of the Steidel et al. (2003) survey have SFRs of $\sim 50 - 100 h_{70}^{-2} M_\odot \text{ yr}^{-1}$ after an average factor of ~ 7 attenuation by dust (Shapley et al. 2003). As previously mentioned, the spectrum of SDSS J1432-0001 is somewhat redder than that of the LBG composite, implying a large correction for dust, and so the SFR could be as much as a few thousand $M_\odot \text{ yr}^{-1}$. With a SFR this large, it would be expected that there would be differences between the spectrum of such an object and its much less active counterparts.

In viewing the spectrum, it is obvious that this object could not be a normal AGN. However, there is the possibility that it is some heretofore unknown form of broad absorption line (BAL) quasar. The line widths are broader in SDSS J1432-0001 than in the composite spectrum, and the luminosity is much higher. However, the widths of these lines are not outside the limits allowed by star formation models such as STARBURST99 (Leitherer et al. 1999), and such a high degree of similarity to the composite spectrum would be remarkable for a BALQSO. As the area covered by Lyman break surveys is very small compared to the area covered by Sloan - only 0.38 deg^2 in the $z \sim 3$ survey by (Steidel et al. 2003) - it is highly likely that SDSS J1432-0001 is simply a very rare, extremely bright LBG with a high SFR.

4. Conclusions

We have searched 1082 quasars in the SDSS EDR catalog for nitrogen-rich objects similar to Q0353-383. Sixteen candidates were found, five of which have stronger nitrogen emission than the others (SDSS J1308–0050, SDSS J1327+0035, SDSS J1744+5351, SDSS J2326–0020, and SDSS J2336–0017), but none with the strength of nitrogen emission from both N IV] $\lambda 1486$ and N III] $\lambda 1750$ that is seen in Q0353-383. Additionally, we found 23 objects with unusual emission or absorption-line properties in our search for objects with weak C IV emission relative to Ly α + N V, one of which appears to be a LBG with an extremely high SFR of $\sim 390 \text{ M}_{\odot} \text{ yr}^{-1}$, without corrections for dust.

Further observations will be necessary in order to determine conclusively whether any of these QSOs do indeed have extreme nitrogen abundances. The best candidates for follow-up observations are J1308-0050, J1327+0035, J1744+5351, J2326-0020, and J2336-0017, as they have the most prominent nitrogen emission lines of the sample and show evidence of both N III] and N IV] emission. Higher S/N data would allow for more precise measuring of equivalent widths. Additionally, the wavelength range of the spectra may be pushed further into the blue, allowing for measurements of Ly α and N V on several of quasars with $z \approx 2$. With better measurements of the line intensities, especially in the seven objects with prominent O III] and He II emission, estimates of the metallicities could be made using several different line ratios, such as N III]/O III], N III]/C III], and N V/He II. These metallicity estimates would allow us to test the hypothesis that nitrogen-rich quasars are exhausting their fuel supply and approaching the metallicities expected by numerical simulations for black holes as they end their quasar phase.

Searches through subsequent SDSS databases will also be necessary to statistically determine the fraction of quasars that fit into the “nitrogen-loud” category and to ascertain the portion of a quasar’s lifetime that is spent in this last, high-metallicity stage before the gas supply is exhausted. It is worth mentioning that any estimate of the frequency of occurrence of these high-metallicity objects may only be a lower limit, however, as both N IV] $\lambda 1486$ and N III] $\lambda 1750$ are collisionally de-excited at densities greater than 10^{11} cm^{-3} (Hamann 1999). There may also exist high-metallicity objects with only N V visible in their spectra, which would be overlooked in our search.

Of the SDSS EDR objects we searched, only three to five of these objects could seriously be considered candidate “nitrogen-loud” quasars, or $\sim 0.4\%$ of the sample of 1082 quasars. The other 12 of the sample of 1082 quasars, or $\sim 1.1\%$, would more appropriately be labeled “nitrogen-salient” objects in that they have noticeable nitrogen emission, but not to the extent of Q0353-383. “Nitrogen-salient” objects may turn out to be valuable as well in that they may help to map out the rapid chemical evolution stages of quasars as the fuel supply is processed through stars. While the above statistics are very rough due to the inhomogeneity of the EDR sample, they do give a guideline measurement of the frequency of such quasars based on a factor of ten larger sample size than the previous estimate by Osmer (1980). We plan to search the SDSS First Data Release database (Abazajian et al. 2003), using the strategies developed in this paper, to improve these

statistics.

We would like to thank Brad Peterson and Rick Pogge for their helpful comments and suggestions, and an anonymous referee for very thorough feedback. Misty Bentz is supported by a graduate fellowship of The Ohio State University.

Funding for the creation and distribution of the SDSS Archive has been provided by the Alfred P. Sloan Foundation, the Participating Institutions, the National Aeronautics and Space Administration, the National Science Foundation, the U.S. Department of Energy, the Japanese Monbukagakusho, and the Max Planck Society. The SDSS Web site is <http://www.sdss.org/>.

The SDSS is managed by the Astrophysical Research Consortium (ARC) for the Participating Institutions. The Participating Institutions are The University of Chicago, Fermilab, the Institute for Advanced Study, the Japan Participation Group, The Johns Hopkins University, Los Alamos National Laboratory, the Max-Planck-Institute for Astronomy (MPIA), the Max-Planck-Institute for Astrophysics (MPA), New Mexico State University, University of Pittsburgh, Princeton University, the United States Naval Observatory, and the University of Washington.

REFERENCES

- Abazajian, K., et al. 2003, AJ, in press (astro-ph/0305492)
- Baldwin, J. A., Hamann, F., Korista, K. T., Ferland, G. J., Dietrich, M., & Warner, C. 2003, ApJ, 583, 649
- Barbaro, G., & Poggianti, B. M. 1997, A&A, 324, 490
- Barkhouse, W. A., & Hall, P. B. 2001, AJ, 121, 2843
- Bolton, J. G., & Wall, J. V. 1970, Australian Journal of Physics, 23, 789
- Boyle, B. J., Fong, R., Shanks, T., & Peterson, B. A. 1990, MNRAS, 243, 1
- Chaffee, F. H., Foltz, C. B., Hewett, P. C., Francis, P. A., Weymann, R. J., Morris, S. L., Anderson, S. F., & MacAlpine, G. M. 1991, AJ, 102, 461
- Chen, Y., Han, J.-L., & He, X.-T. 2000, Acta Astrophysica Sinica, 20, 366
- Hamann, F. 1999, in ASP Conf. Ser. 162: Quasars and Cosmology, 409
- Hamann, F., & Ferland, G. 1999, ARA&A, 37, 487
- Hewett, P. C., Foltz, C. B., Chaffee, F. H., Francis, P. J., Weymann, R. J., Morris, S. L., Anderson, S. F., & MacAlpine, G. M. 1991, AJ, 101, 1121

- Hewitt, A., & Burbidge, G. 1987, *ApJS*, 63, 1
- Huang, K.-L., & Usher, P. D. 1984, *ApJS*, 56, 393
- Kennicutt, R. C. 1998, *ARA&A*, 36, 189
- La Franca, F., Gregorini, L., Cristiani, S., de Ruiter, H., & Owen, F. 1994, *AJ*, 108, 1548
- Leitherer, C., Schaerer, D., Goldader, J. D., Delgado, R. M. G., Robert, C., Kune, D. F., de Mello, D. F., Devost, D., & Heckman, T. M. 1999, *ApJS*, 123, 3
- MacAlpine, G. M., Lewis, D. W., & Smith, S. B. 1977, *ApJS*, 35, 203
- Morton, D. C. 1991, *ApJS*, 77, 119
- Osmer, P. S. 1980, *ApJ*, 237, 666
- Osmer, P. S., Porter, A. C., & Green, R. F. 1994, *ApJ*, 436, 678
- Osmer, P. S., & Smith, M. G. 1980, *ApJS*, 42, 333
- Perlman, E. S., Padovani, P., Giommi, P., Sambruna, R., Jones, L. R., Tzioumis, A., & Reynolds, J. 1998, *AJ*, 115, 1253
- Richards, G. T., et al. 2002, *AJ*, 123, 2945
- Schneider, D. P., et al. 2002, *AJ*, 123, 567
- Shapley, A. E., Steidel, C. C., Pettini, M., & Adelberger, K. L. 2003, *ApJ*, 588, 65
- Simard-Normandin, M., Kronberg, P. P., & Button, S. 1981, *ApJS*, 46, 239
- Sirola, C. J., Turnshek, D. A., Weymann, R. J., Monier, E. M., Morris, S. L., Roth, M. R., Krzeminski, W., Kunkel, W. E., Duhalde, O., & Sheaffer, S. 1998, *ApJ*, 495, 659
- Steidel, C. C., Adelberger, K. L., Shapley, A. E., Pettini, M., Dickinson, M., & Giavalisco, M. 2003, *ApJ*, 592, 728
- Stoughton, C., et al. 2002, *AJ*, 123, 485
- Véron-Cetty, M.-P., & Véron, P. 2001, *A&A*, 374, 92
- Vanden Berk, D. E., et al. 2001, *AJ*, 122, 549
- Visnovsky, K. L., Impey, C. D., Foltz, C. B., Hewitt, P. C., Weymann, R. J., & Morris, S. L. 1992, *ApJ*, 391, 560
- York, D. G., et al. 2000, *AJ*, 120, 1579

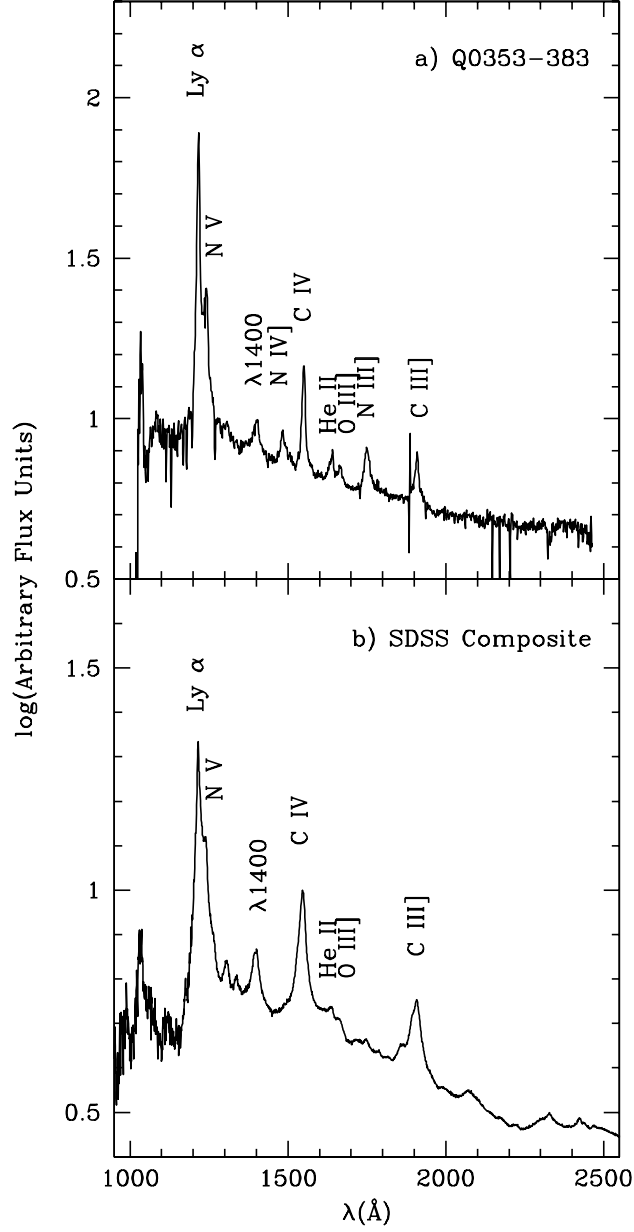


Fig. 1.— Rest frame spectrum of Q0353-383 (Baldwin, private communication), and the SDSS composite (Vanden Berk et al. 2001), composed of 2204 QSO spectra from 66 spectroscopic plates. Both spectra are plotted in semi-log format to enhance fine details.

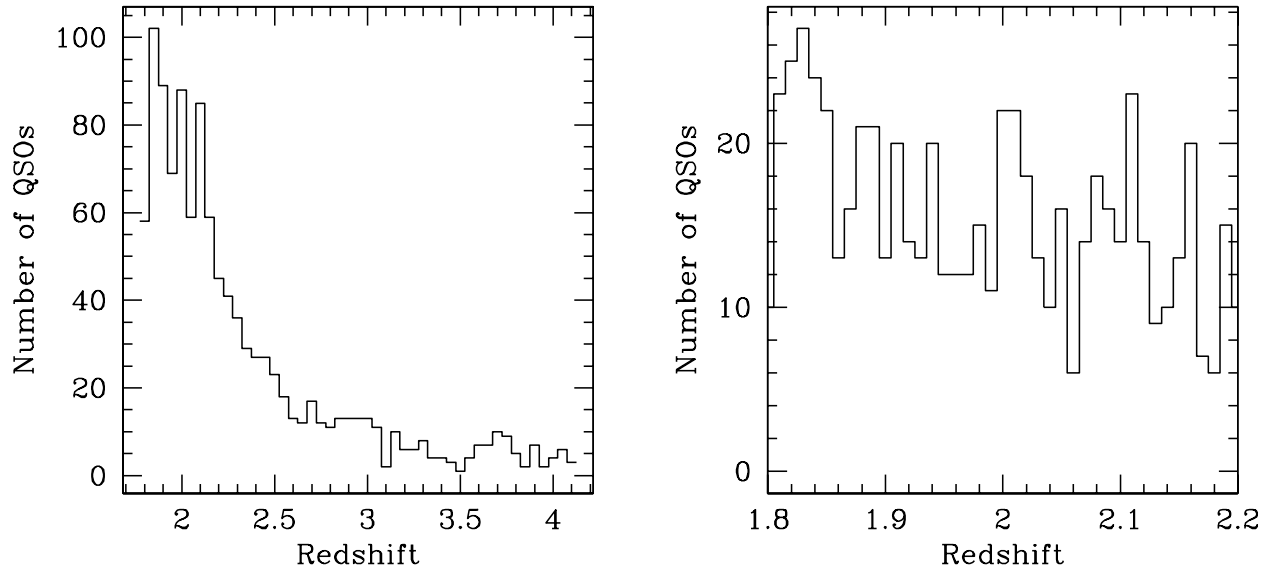


Fig. 2.— Redshift distribution for the 1082 objects in the SDSS EDR with $1.8 < z < 4.1$ and bin size $\Delta z = 0.05$, and distribution centered around $z = 2$ with bin size $\Delta z = 0.01$.

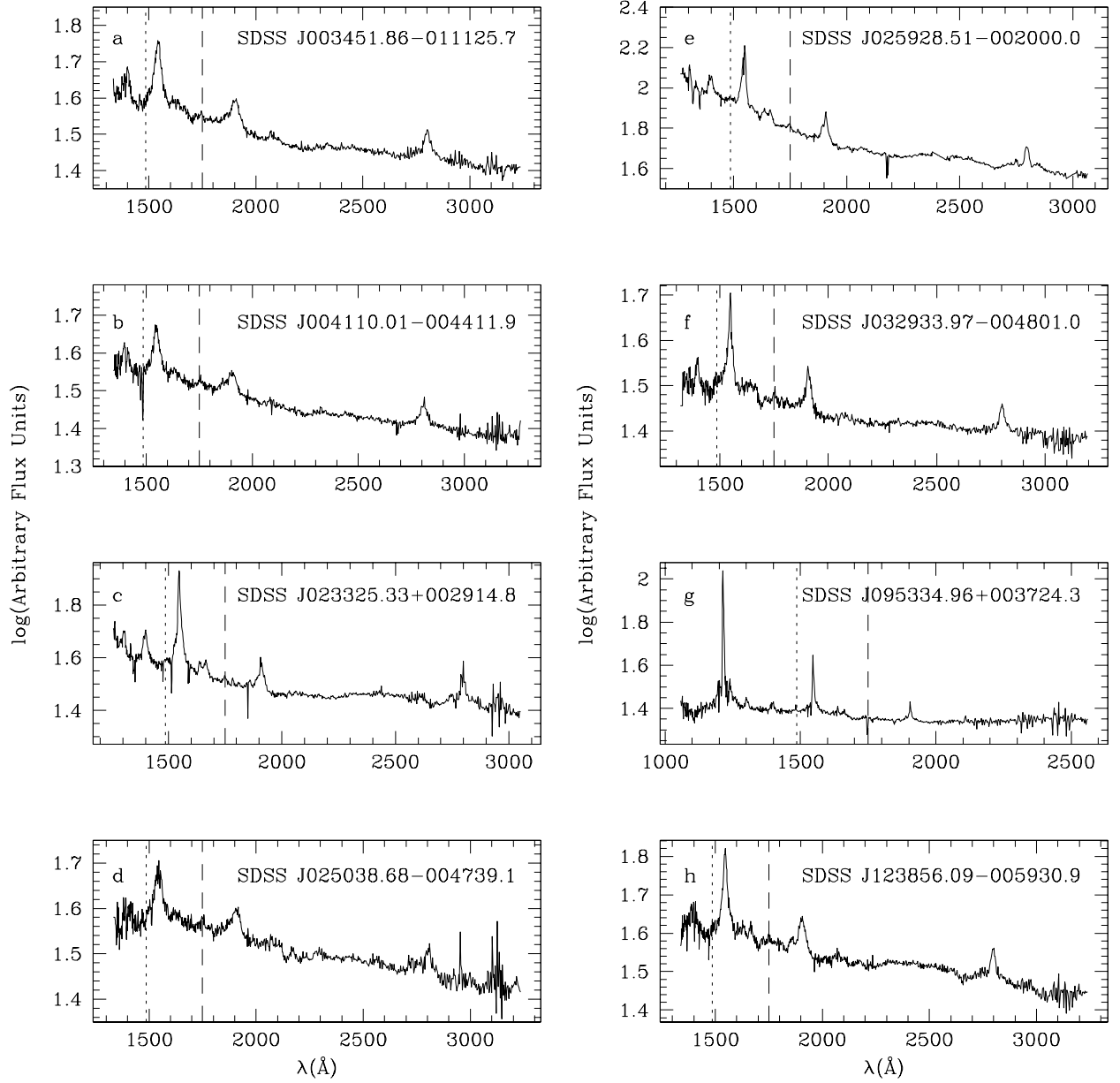
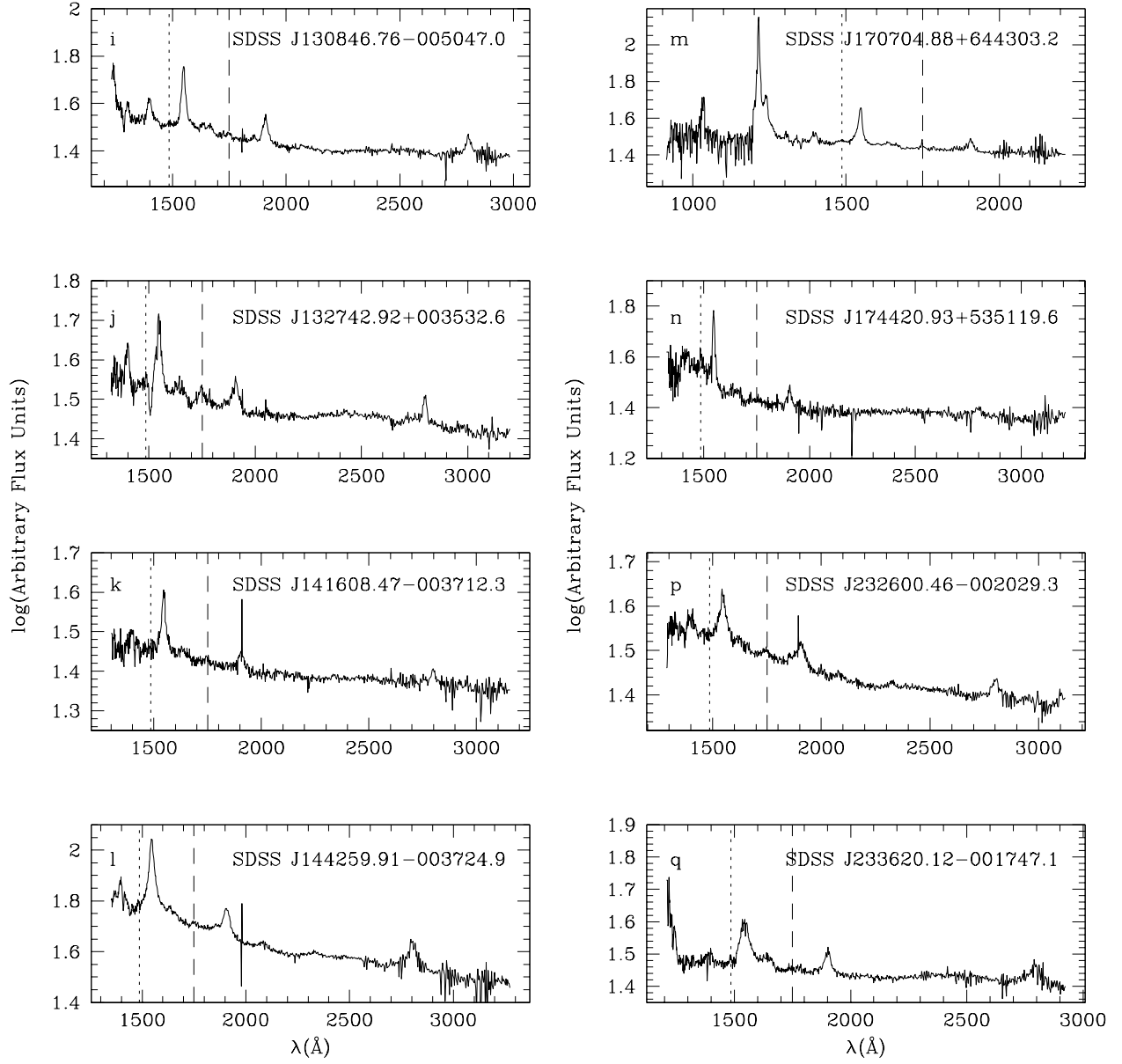


Fig. 3.— Rest frame spectra of the 16 nitrogen enriched candidate QSOs from the SDSS EDR database. The spectra are smoothed with a bin of five pixels and plotted in semi-log format to enhance fine details. The dotted line is at N IV] $\lambda 1486$ Å and the dashed line is at N III] $\lambda 1750$ Å.



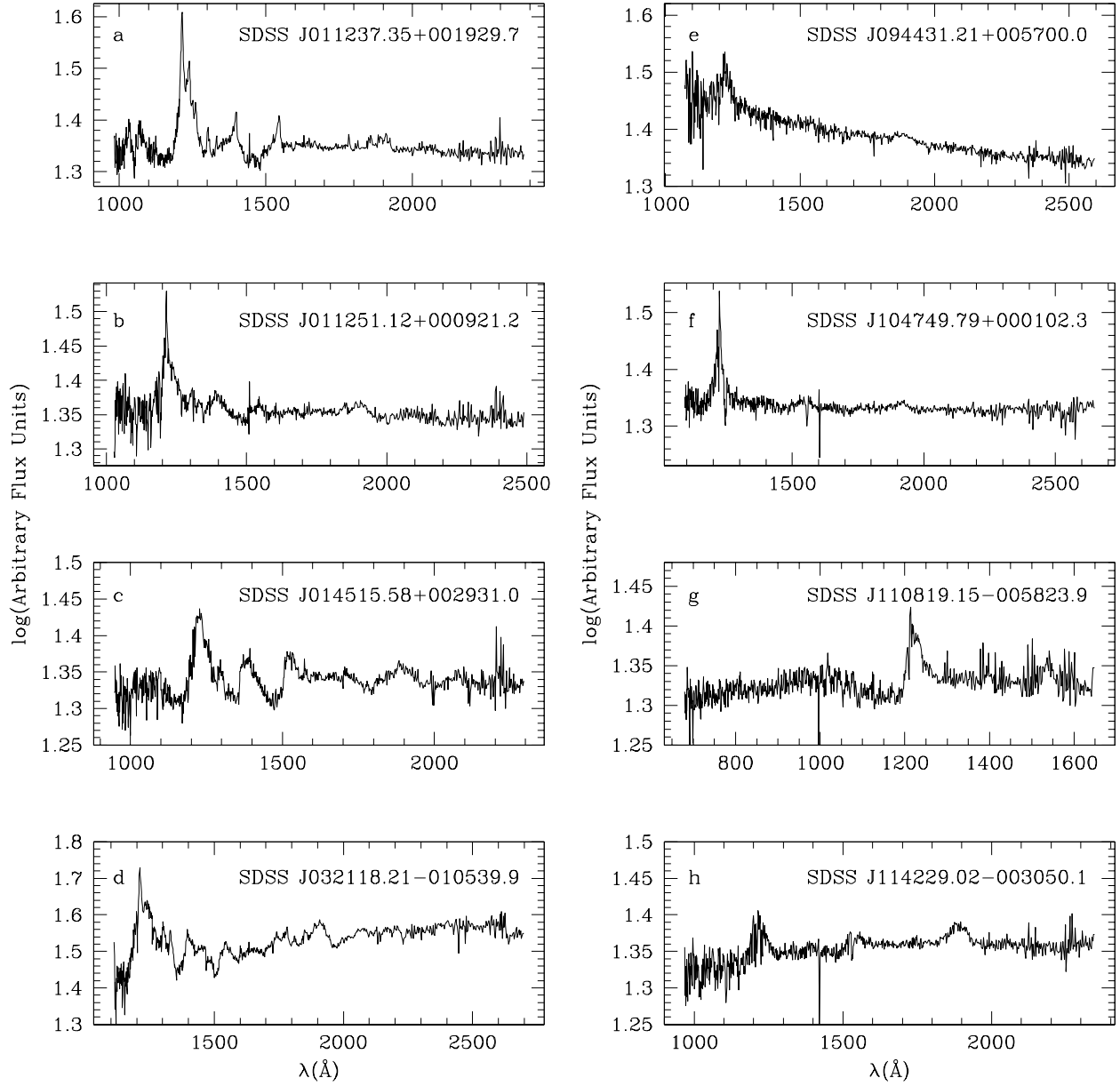
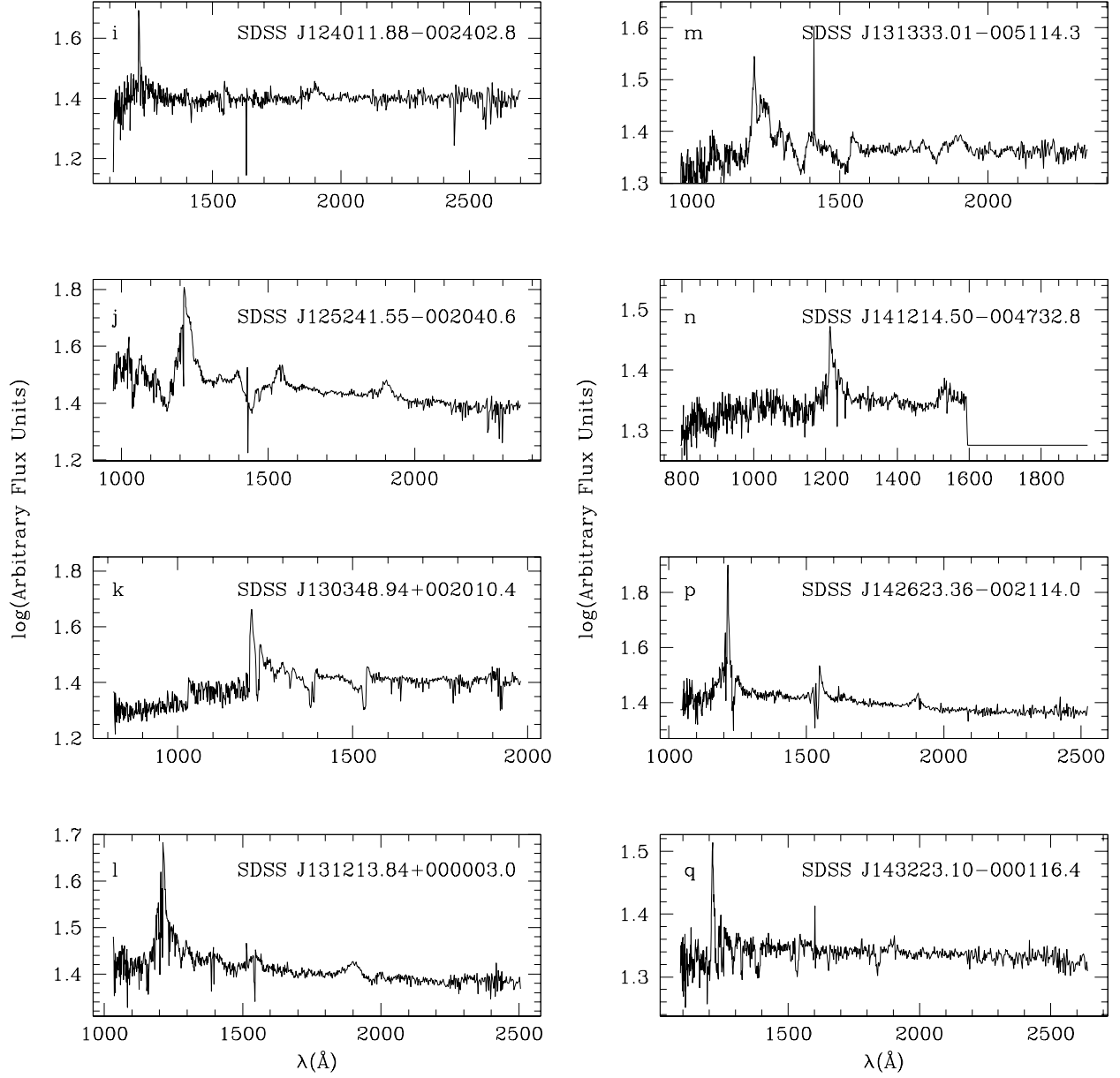
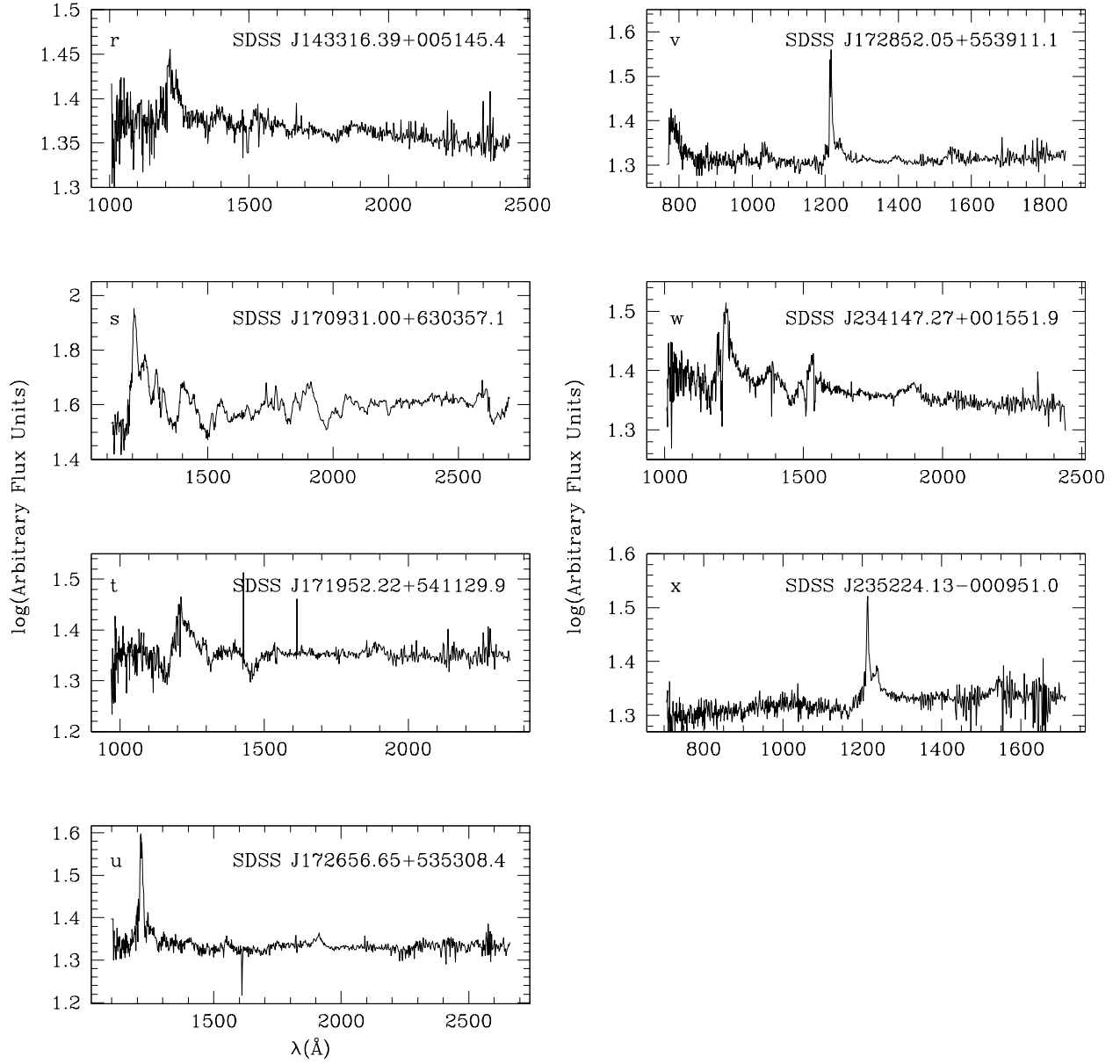


Fig. 4.— Rest frame spectra of the 23 unusual quasars. The spectra are smoothed with a bin of five pixels and plotted in semi-log format to enhance fine details.





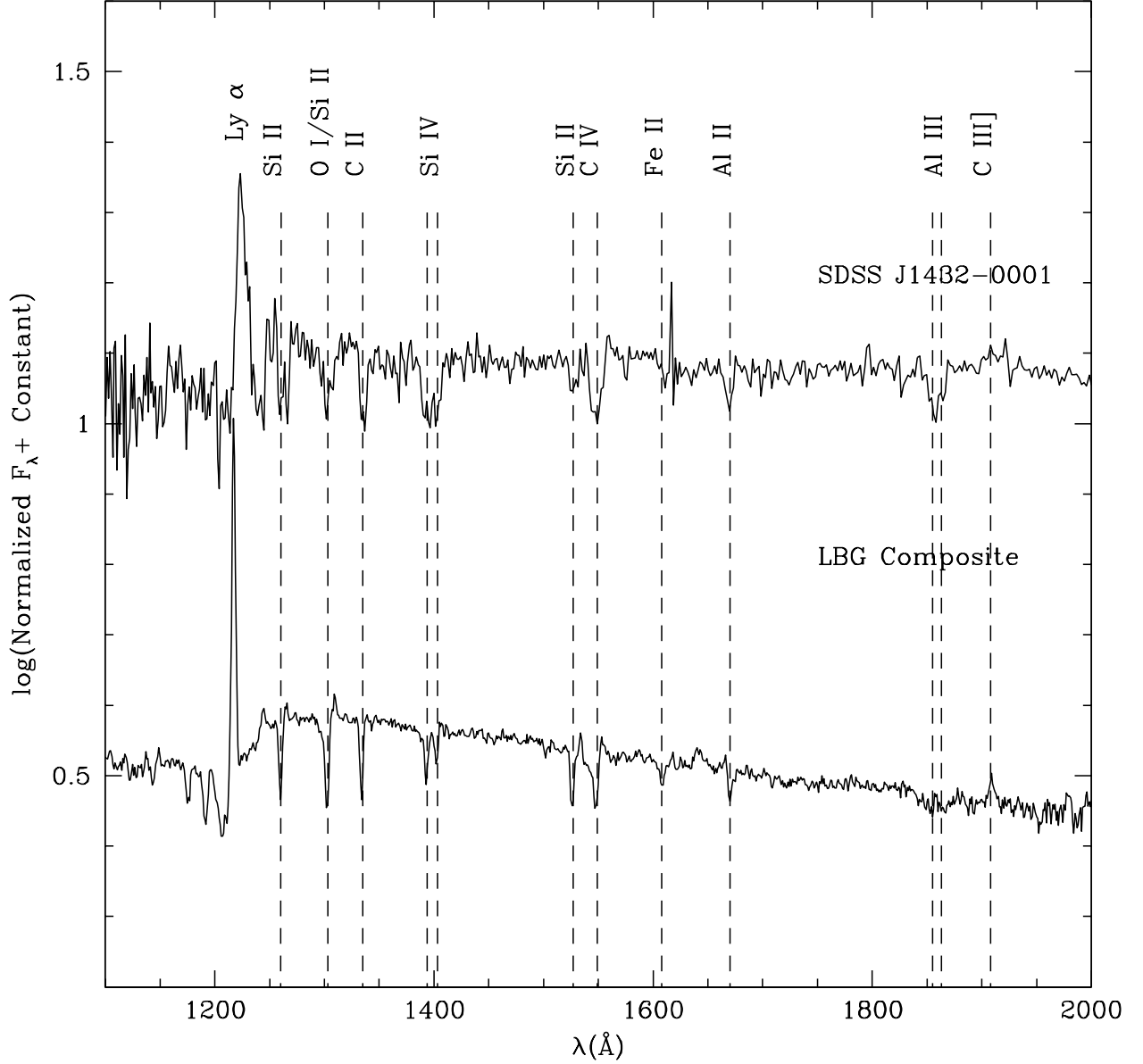


Fig. 5.— Comparison of rest frame composite spectrum, made up of 811 individual Lyman break galaxies (Shapley et al. 2003), and Sloan object SDSS J1432-0001. The Sloan spectrum was smoothed with a bin of five pixels, and both spectra are plotted in semi-log space to enhance fine details.

Table 1. Properties of Nitrogen Enriched Candidate Quasars

QSO	z^a	i* Magnitude ^a		Add. Identifier	Notes ^b	References ^c
		Obs.	Abs.			
SDSS J003451.86–011125.7	1.846	18.13	-27.07	UM 259	L3	10, 11, 15
SDSS J004110.00–004411.8	1.819	18.35	-26.81			
SDSS J023325.33+002914.9	2.014	18.12	-27.26			
SDSS J025038.68–004739.1	1.845	18.10	-27.17	US 3221	RQ	8, 9, 15
SDSS J025928.52–002000.0	2.002	16.98	-28.54	PKS 0256-005	RL, FSRQ, L1	1, 2, 4, 7, 11, 12, 13, 15
SDSS J032933.97–004801.2	1.880	18.55	-26.85			
SDSS J095334.96+003724.5	2.606	19.19	-26.77			
SDSS J123856.10–005930.9	1.848	17.95	-27.25	QNY4:41	RD, L2	3, 5, 6, 15
SDSS J130846.76–005046.9	2.087	18.85	-26.60			
SDSS J132742.92+003532.6	1.876	18.34	-26.89			
SDSS J141608.47–003712.3	1.921	18.98	-26.34			
SDSS J144259.91–003724.9	1.818	17.51	-27.69	LBQS 1440-0024	RQ, OSV, L4	6, 14, 15, 16
SDSS J170704.88+644303.3	3.168	18.42	-27.90			
SDSS J174420.94+535119.5	1.864	19.63	-25.62			
SDSS J232600.47–002029.3	1.946	18.58	-26.76			
SDSS J233620.13–001747.1	2.146	18.35	-27.19			

^aAs determined by Schneider et al. (2002), with $H_0 = 50$, $\Omega_M = 1$, $\Omega_\Lambda = 0$, and $\alpha_Q = 0.5$

^b**Abbreviations:** RL = Radio Loud; RD = Radio Detected; RQ = Radio Quiet; L1 = strong, well-separated Ly α and N V; L2 = strong, separated Ly α and N V; L3 = broad Ly α ; L4 = narrow Ly α , N V indistinguishable; FSRQ = Flat Spectrum Radio Quasar; OSV = Optically Strong Variable

^cThis research has made use of the NASA/IPAC Extragalactic Database (NED) which is operated by the Jet Propulsion Laboratory, California Institute of Technology, under contract with the National Aeronautics and Space Administration.

References. — 1. Barkhouse & Hall (2001); 2. Bolton & Wall (1970); 3. Boyle et al. (1990); 4. Chaffee et al. (1991); 5. Chen et al. (2000); 6. Hewett et al. (1991); 7. Hewitt & Burbidge (1987); 8. Huang & Usher (1984); 9. La Franca et al. (1994); 10. MacAlpine et al. (1977); 11. Osmer et al. (1994); 12. Perlman et al. (1998); 13. Simard-Normandin et al. (1981); 14. Sirola et al. (1998); 15. Véron-Cetty & Véron (2001); 16. Visnovsky et al. (1992).

Table 2. Measured Equivalent Widths N IV] λ 1486 and N III] λ 1750

QSO	SNR	N IV]		N III]		CCC ^a	
		W_{obs} (Å) ^b	σ^c	W_{obs} (Å) ^b	σ^c	λ 1486 Å	λ 1750 Å
Q0353–383 ^d	...	5.0	...	9.0	...	0.98	0.99
SDSS J0034–0111	15	3.0	8.2	0.04	0.72
SDSS J0041–0044	14	5.0	12.8	0.01	0.75
SDSS J0233+0029	15	3.0	8.2	0.34	0.85
SDSS J0250–0047	14	3.0	7.7	0.29	0.67
SDSS J0259–0020	39	1.0	7.1	0.80	0.91
SDSS J0329–0048	9	5.0	8.2	0.15	0.82
SDSS J0953+0037	9	1.0	1.6	... ^e	...	0.58	0.02
SDSS J1238–0059	22	2.0	8.0	0.02	0.64
SDSS J1308–0050	7	1.0	1.3	3.5	4.5	INDEF ^f	0.79
SDSS J1327+0035	10	1.5	2.7	12.0	21.9	0.18	0.93
SDSS J1416–0037	7	4.0	5.1	0.03	0.65
SDSS J1442–0037	26	2.0	9.5	0.01	0.73
SDSS J1707+6443	19	... ^g	...	3.0	10.4	0.61	0.57
SDSS J1744+5351	4	7.0	5.1	1.5	1.1	0.74	0.10
SDSS J2326–0020	11	1.0	2.0	4.0	8.0	0.00	0.68
SDSS J2336–0017	13	3.0	7.1	2.0	4.7	0.57	0.32

^g Obstructed by Fe emission

^aCross-correlation coefficients for the 30 Å windows as described in the text; auto-correlation coefficients for Q0353-383

^bGuideline measurements, with errors of 0.5-1.0 Å

^cSignificance of detection, assuming a 30 Å window

^dValues taken from Baldwin et al. (2003)

^eObstructed by [O I] sky line

^fIRAF fit did not converge

Table 3. Measured Equivalent Widths He II $\lambda 1640$ and O III] $\lambda 1664$

QSO	W_{obs} (Å) ^a	
	He II	O III]
Q0353–383	4.0	2.0
SDSS J0034–0111	3.6	3.0
SDSS J0233+0029	4.7	5.7
SDSS J0259–0020	9.6	4.4
SDSS J0953–0037	1.6	1.0
SDSS J1238–0059	...	5.6
SDSS J1308–0050	2.5	2.5
SDSS J1442–0037	2.0	0.6

^aGuideline measurements, with errors of 0.5-1.0 Å

Table 4. Properties of Quasars with Small C IV/(Ly α + N V)

QSO	z^a	R^b	i* Magnitude ^a		Characteristics
			Observed	Absolute	
SDSS J011251.12+000921.2	2.865	0.096	19.70	-26.42	strong, narrow Ly α , well separated N V
SDSS J011237.35+001929.7	2.695	0.081	19.60	-26.40	broad and narrow Ly α components
SDSS J014515.58+002931.0	3.006	0.077	19.87	-26.35	BAL quasar
SDSS J032118.21–0010539.9	2.412	0.044	17.61	-28.25	BAL quasar
SDSS J094431.21+005700.0	2.550	0.081	19.30	-26.75	slope to blue and broad, weak emission lines
SDSS J104749.79+000102.3	2.479	0.066	19.99	-25.85	narrow, intrinsic C IV and N V absorption
SDSS J110819.15–005823.9	4.560	0.047	19.89	-27.19	broad Ly α
SDSS J114229.02–003050.0	2.927	0.007	19.50	-26.64	slope to red and broad, strong emission lines
SDSS J124011.88–002402.8	2.417	0.091	19.29	-26.47	narrow, intrinsic C IV and N V absorption
SDSS J125241.55–002040.6	2.898	0.010	18.53	-27.61	BAL quasar
SDSS J130348.94+002010.4	3.655	0.057	18.72	-27.87	multiple P-Cygni lines (C IV, N V, Si λ 1400, etc.)
SDSS J131213.84+000003.0	2.681	0.043	18.89	-27.10	narrow, intrinsic C IV and N V absorption
SDSS J131333.01–005114.3	2.949	0.077	19.16	-27.00	BAL quasar
SDSS J141214.50–004732.8	3.777	0.073	19.82	-26.90	narrow, intrinsic C IV and N V absorption
SDSS J142623.36–002114.0	2.644	0.000	19.23	-26.74	narrow, intrinsic C IV and N V absorption
SDSS J143223.10–000116.4	2.483	0.056	20.12	-25.73	high redshift star-forming galaxy
SDSS J143316.39+005145.4	2.774	0.096	19.61	-26.45	BALs and narrow, intrinsic C IV absorption
SDSS J170931.00+63.0357.1	2.402	0.034	17.31	-28.44	BAL quasar
SDSS J172656.65+535308.4	2.905	0.029	19.70	-26.47	BALs and narrow, intrinsic C IV absorption
SDSS J172852.05+553911.2	2.461	0.083	20.21	-25.62	broad and narrow Ly α components
SDSS J234147.27+001551.9	3.950	0.079	20.03	-26.73	strong, narrow Ly α , well separated N V
SDSS J235224.13–000951.0	2.769	0.042	19.24	-26.81	BALs and narrow, intrinsic C IV absorption
SDSS J235718.36+004350.3	4.340	0.073	19.87	-27.09	strong, narrow Ly α , well separated N V

^aAs determined by Schneider et al. (2002), with $H_0 = 50$, $\Omega_M = 1$, $\Omega_\Lambda = 0$, and $\alpha_Q = 0.5$

^bRatio of C IV/(Ly α + N V), calculated using the equivalent widths of the emission lines determined by the SDSS pipeline